Simulation of PMSM Vector Control Based on a Self-tuning Fuzzy PI Controller

Yuan Zhou, Wendong Shang, Mingshan Liu[1†], Xiaokun Li and Ying Zeng
College of Communication Engineering
Jilin University
Changchun,130012, China
shangwend@sina.com

***Abstract*—PMSM vector control system with a proportional-integral (PI) controller exists some defects such as slow speed response, large torque ripple and poor anti interference ability. A new fuzzy PI control method with adjustable proportion factor (APFPI) is proposed in this paper. The proportion factor can be adjusted by RBF neural network (RBFNN) online. In the PMSM vector control system, the current loop will be adjusted by a PI controller and the speed loop will be adjusted by an APFPI controller. The simulation results show that the speed and torque response of PMSM vector control system with APFPI controller has better control performance.**

Keywords- PMSM vector control; Fuzzy control; RBFNN.

I. INTRODUCTION

The permanent magnet synchronous motor (PMSM) has many advantages such as wide speed range, light weight, small size, low rotational inertia, small torque ripple, and so on. PMSM has been widely used in industry, agriculture, aerospace and other fields [1].

Although PMSM has so many advantages, it is difficult to achieve the precious control of PMSM speed, as it is a nonlinear control system and strong coupling among the rotor speed and the winding currents. In order to facilitate the research of PMSM, researchers have proposed two typical control methods: vector control and direct torque control [2].

Generally, the PI controllers are used in speed and current closed-loop in PMSM control system. However, the conventional PI controllers have disadvantages such as slow speed response, large torque ripple. Different methods are proposed to make the PMSM vector control system has good dynamic response performance, such as adaptive PID controller [3], adaptive-network-based fuzzy PI controller [4], neuro-wavelet-based PI controller [5], sliding-mode controller, nonlinear adaptive backstepping controller [6-7] and others.

The fuzzy PI (FPI) controller has been applied successfully in PMSM control. In many works, using fuzzy logic and neural network to obtain the adequate parameters of PI controller is proposed [8-10]. In the FPI controller, the proportion factor plays an important role. But the conventional FPI controller uses a fixed proportion factor in general. In this paper, the APFPI controller which has self-turning proportion factor is proposed. The simulation model of PMSM vector control system will be set up in matlab/simulink. The current loop is controlled by a conventional PI controller and the speed loop is controlled by an APFPI controller. The simulation results demonstrate that the APFPI controller has good control performance for the speed and torque control.

† *Corresponding Author: Mingshan Liu, Associate Professor, College of Communication Engineering, Jilin University*

II. MATHEMATICAL MODEL OF PMSM

The theory of PMSM vector control method is described as follows: in static reference frame (*abc*) the 3 different stator currents vectors can be decomposed into 2 independent phase current components in rotor reference frame (*dq*) using Park and Clark coordinate transformation. Then a PMSM's mathematical model can be expressed as following equations.

1) Voltage equations

The voltage equations of PMSM in rotor reference frame can be express as follows:

$$\begin{cases} u_d = R_s i_d + L_d \dfrac{\mathrm{d}i_d}{\mathrm{d}t} - n_p \omega L_q i_q \\ u_q = R_s i_q + L_q \dfrac{\mathrm{d}i_q}{\mathrm{d}t} + n_p \omega L_d i_d + n_p \omega \Phi \end{cases} \tag{1}$$

2) Torque equation

The torque equation of PMSM in rotor reference frame can be express as follows:

$$\tau = \frac{3}{2} n_p [(L_d - L_q) i_d i_q + \Phi i_q] \tag{2}$$

3) motion equation

The motion equation of PMSM can be express as follows:

$$\tau = J \frac{\mathrm{d}\omega}{\mathrm{d}t} + \tau_L + B\omega \tag{3}$$

where Rs is the winding resistance of per phase, L_d and L_q are the d-q axis' inductances, i_d and i_q are the d-q axis' currents, n_p is the pair number of motor poles, ω is the rotor electrical speed. J is the rotational inertia, τ is the motor output torque, τ_L is the load torque, B is the damping co-efficient.

In order to accomplish the maximum torque and the maximum efficiency and make the PMSM has linear characteristics, i_d is defined $i_d = 0$ and using the surface PMSM ($L_d = L_q$), the PMSM model in d-q axis can be simplified as follows:

$$\tau = n_p \Phi i_q \tag{4}$$

Equation (4) shows that the motor output torque τ and the q-axis current i_q are linear relations. Therefore, the PMSM control method is similar to the DC motor control method.

III. PRINCIPLE OF PMSM VECTOR CONTROL SYSTEM

A typical structure block diagram of PMSM vector control system with two closed-loops is shown in Figure 1[5]. As the PI controller has simple structure and extensive application, the current and the speed closed-loop are generally controlled by PI controllers. There are four modules in this control system: PMSM module, 3-phase inverter module, coordinate transformation module and SVPWM module etc. .

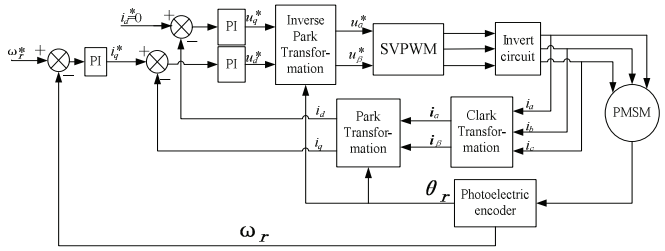

Figure 1 Structure block diagram of PMSM vector control system

In Figure 1, ω_r^* is the reference speed, i_d^* is the d-axis reference current, and i_q^* is the q-axis reference current. PMSM vector control system is described as follows: Adopt speed deviation $\Delta\omega$ as input value, and then PI controller will output i_q^*, which is the reference value of the q-axis current loop. In inner current loop, i_d and i_q which can be obtained from the three phase current i_a , i_b and i_c are transformed through Clark coordinate transformation and Park coordinate transformation are the current loop feedback. The PI controller in inner loop will output u_d^* and u_q^*, which are the reference value of the iPark(inverse Park) coordinate transformation. SVPWM control signals can be generated through u_α^* and u_β^*, which are the outputs of iPark coordinate transformation. SVPWM control signals will control the three phase voltage inverter to drive PMSM.

IV. THE FUZZY PI CONTROLLER WITH AJUSTABLE PROPORTION FACTOR

A. Fuzzy controller structure

The fuzzy controller is implemented depending on the experts' experience. It doesn't need to provide the precise mathematical model of a control system. Therefore it is widely used to improve dynamic performance of a nonlinear or an uncertain system [11].

1) The scheme block of Fuzzy PI controller.

The scheme block of speed loop control system with a FPI controller is shown in Figure 2. This FPI controller has two inputs and one output. One input is the speed error e, and the other is the speed change of error ec. The output is the incremental of proportion factor.

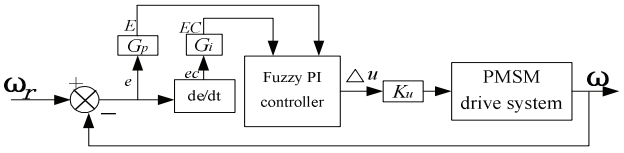

Figure 2. Fuzzy PI controller structure diagram

In Figure 2, ω_r is the command speed, ω is the feedback speed of PMSM, Δu is the output of fuzzy logic controller, it represent the increment of i_q. G_P and G_i are quantitative factors. K_u is proportion factor, and it directly affects the gain of the entire system. E and EC correspond to the fuzzy variables. They can be defined:

$$\begin{cases} E = G_p \times e \\ EC = G_i \times ec \end{cases} \tag{5}$$

By the equation (5), e and ec can be transformed from the practical domain to the fuzzy domain.

2) Fuzzy reasoning and fuzzy rules.

For the inputs e and ec in practical domain, the value of e ranges from {-2000, 2000}, and the value of ec ranges from {-100, 100}. In fuzzy domain, E and EC are defined in {-6, 6}, and they are divided into seven members i.e. E={NB, NM, NS, ZO, PS, PM, PB}, EC={NB, NM, NS, ZO, PS, PM, PB}. The membership function graph of E and EC are shown in Figure 3.

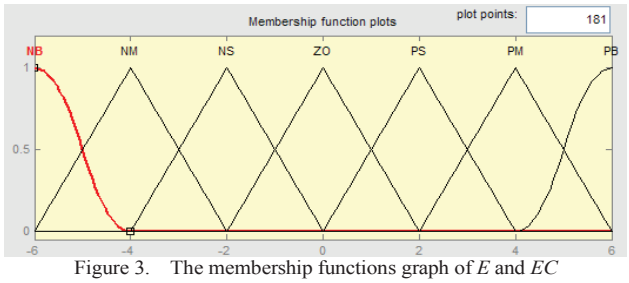

Figure 3. The membership functions graph of E and EC

Similarly, the value of fuzzy logic controller output Δu range from {-4, 4}. Δu has seven membership functions i.e. Δu ={NB, NM, NS, ZO, PS, PM, PB}. Figure 4 shows the membership function graph of Δu .

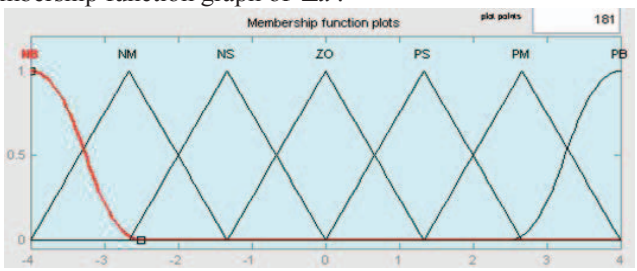

Figure 4. The membership functions graph of Δu

Depending on the signals E and EC, the fuzzy controller automatically adjusts the output Δu based on the fuzzy control rules [12].

The rule base is defined with the structure of a rule given by equation (6).

If (*e* is A_i) **and** (*ec* is B_j) **then** (Δu is C_m) (6)

where *i*=0,l, … 7, *j*=0,1,…,7, *m*=0,l, … 7.

Based on the basic rule mentioned in equation (6), the control rules of the fuzzy PI controller are established. The fuzzy control rules are shown in table 1.

TABLE I. FUZZY CONTROL RULES

ec	e						
	NB	***NM***	***NS***	***ZO***	***PS***	***PM***	***PB***
NB	ZO	PS	PS	PM	PM	PB	PB
NM	NS	ZO	PB	PB	PB	PB	PB
NS	NM	NS	ZO	PS	PS	PM	PM
ZO	NS	PS	ZO	ZO	NS	NM	NM
PS	NS	NS	PS	ZO	ZO	NS	NS
PM	NM	NM	PS	NS	NS	NS	NS
PB	NB	NB	PS	NM	NM	NM	NS

3) Defuzzification:

The fuzzy controller will output a fuzzy variable. In order to obtain a real domain variable, the defuzzification of fuzzy variable is an important step. By using centroid method to realize the defuzzification, the output will be much smoother. This method can be express as follows [13]:

$$U = \frac{\sum_{i=1}^{n} UF_i \mu(UF_i)}{\sum_{i=1}^{n} \mu(UF_i)} \tag{7}$$

where $\mu(UF_i)$ is the membership degree of *i*th rule, UF_i is the output center of the *i*th rule.

B. RBF neural network

Radial Basis Function (RBF) neural network is proposed in late 1980s. It has widely used in curve fitting, parameter classification and clustering analysis etc. [14].

The typical RBFNN has three layers: input layer, hidden layer and output layer [15]. The input layer will receive the external signals and send them to the hidden layer. Then the hidden layer will calculate the signals and produce the stronger signals. The output layer is usually a simple transformation to combine the output signals of hidden layer. The basic structure RBFNN is shown in Figure 5.

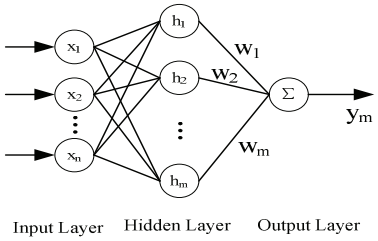

Figure 5. The structure of RBFNN

In the RBFNN structure, $\mathbf{X} = [x_1, x_2, \cdots, x_n]^T$ is the input vector of the RBFNN. $\mathbf{W} = [w_1, w_2, \cdots, w_n]^T$ is the connection weight of hidden layer node and output layer node.

The *j*th hidden layer node's output can be calculated by the Gaussian function:

$$h_j = \exp\{-\frac{\|x - \mu_j\|^2}{2\sigma_j^2}\}, \ j=1,2,\ldots,\mathrm{m} \tag{8}$$

where *x* is the input data, μ_j is the center of the *j*th hidden layer node, σ_j is the width of the *j*th hidden layer node, *m* is the number of hidden layer nodes.

The value of the output node is calculated by:

$$y_m = \sum_{j=1}^{m} w_j h_j \tag{9}$$

C. Fuzzy PI controller with adjustable proportion factor

A large number of experiments have proved that proportion factor in fuzzy controller has great influence on the control system [13], but the proportion factor is set to a fixed value in general. In order to achieve better control effect, a new FPI controller with an adjustable proportion factor is designed. With the change of the speed error, the proportion factor will be tuned by RBFNN.

In theory, RBFNN can approximate the nonlinear function with any accuracy. In this paper, a series of proportion factor data is obtained by experiment, which is used as the input of RBFNN. Before training the network, the fitting accuracy about the proportion factor data should be set, then the RBFNN can automatically adjust the number of nodes in hidden layer, and obtain the parameters' value such as μ_j and σ_j. When the state of PMSM control system is change, the output weights of neural network will adjust the proportion factor on-line.

The scheme block of fuzzy PI control system with adjustable proportion factor is shown in Figure 6.

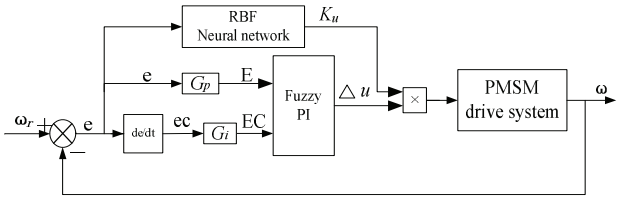

Figure 6. The structure of FPI controller with an adjustable proportion factor

The fitting accuracy about the proportion factor data is set to 0.000001. After the RBFNN is trained, the parameters of RBFNN is as follows: the hidden layer node's number is 29, the weights of hidden layer and output layer are expressed in a vector and the weight vector is **W**=[6, 3, 9, -19, -16, -13, -10, 4, 8, -7, -17, -20, -15, -12, -4, -1, -8, 5, 7, -18, -14, -6, 1, -11, -9, -2, 0, -5, -3]^T. The fitting curve of the proportion factor is shown in Figure 7.

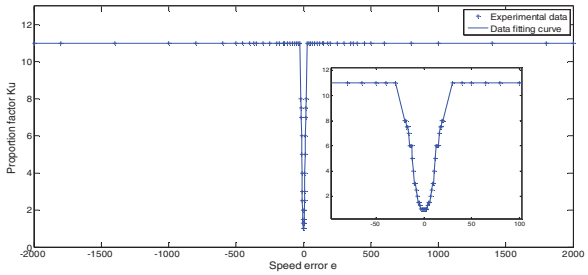

Figure 7. The fitting curve of proportion factor

The proportion factor will be adjusted according to the speed error, and its value will be chosen in the curve in figure 7.

V. SYSTEM SIMULATION AND RESULT ANALYSIS

In matlab/simulink environment, the block diagram of PMSM vector control system with APFPI controller in speed loop is shown in Figure 8. Fuzzy logic toolbox is used to establish the APFPI controller module.

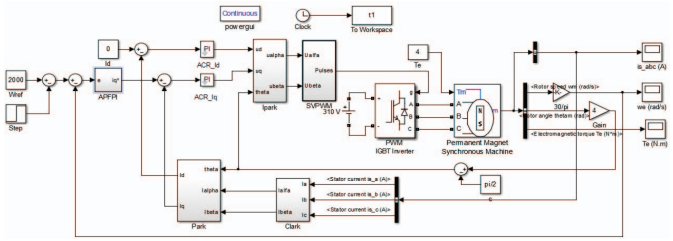

Figure 8. PMSM double closed-loop control system model

The specific description of APFPI module is shown in Figure 9. The S-Function module is provided by the toolbox of matlab/simulink and the RBFNN is built in this module. The input of S-Function is the input of RBFNN, and the output of S-Function is the output of RBFNN.

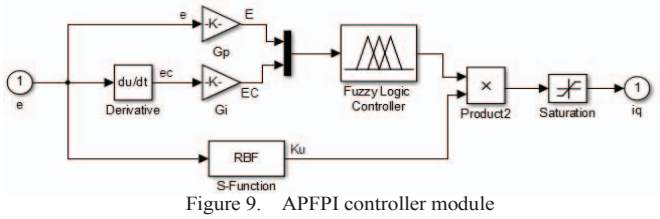

Figure 9. APFPI controller module

The parameters of the PMSM which is used in this system are as follows: stator resistance: $R_s = 1.74\Omega$, *d-q* axis inductance: $L_d = L_q = 0.835\times10^{-3}\,mH$, equivalent flux by the magnets: $\Phi = 0.1176\text{Wb}$, moment of inertia: $J = 0.174\times10^{-4}\,\text{kg}\cdot\text{m}^2$, number of pole pairs: $n_p = 4$, magnetic flux density: $B = 0$, motor rated speed: $\omega = 2310\,\text{rpm}$, motor rated power: P=11kW.

The initial condition of simulation is given as follows: the command speed is 2000rpm, load torque is 4N·m, the simulation time is 0.04s, then the speed will reduce to 1500rpm in 0.02s.

When adopting conventional PI controller and FPI controller in speed loop, the speed response curves are shown in Figure 10.

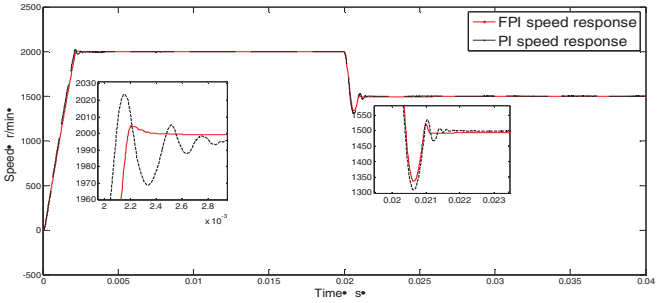

Figure 10. Speed response curve of PI and FPI control system

Figure 10 shows that the speed response of FPI controller has small overshoot and it needs a short time to achieve steady state.

When adopting FPI controller and APFPI controller in speed loop, the speed response curves are shown in Figure 11.

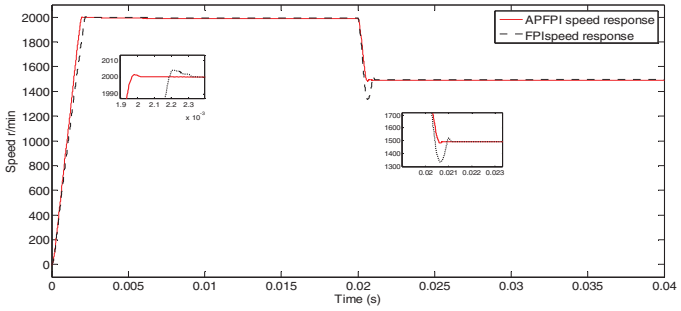

Figure 11. Speed response curve of APFPI and FPI control system

Figure 11 shows that the speed response of APFPI controller has small overshoot and it needs a short time to achieve steady state.

Figure 10 to 11 show that the PMSM vector control system with APFPI controller has the best dynamic behavior. In this system the speed response is fast and the speed tracking performance is good.

The torque response of PMSM vector control system with PI, FPI and APFPI controller have been shown in Figure 12 to 14.

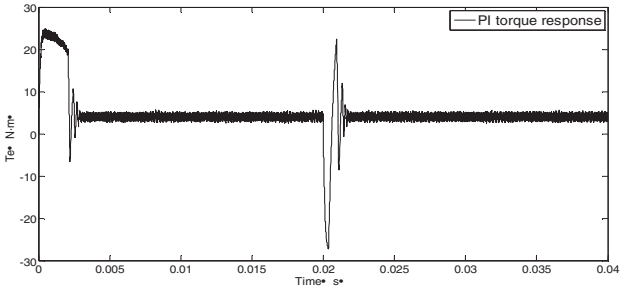

Figure 12. Torque response curve under PI controller

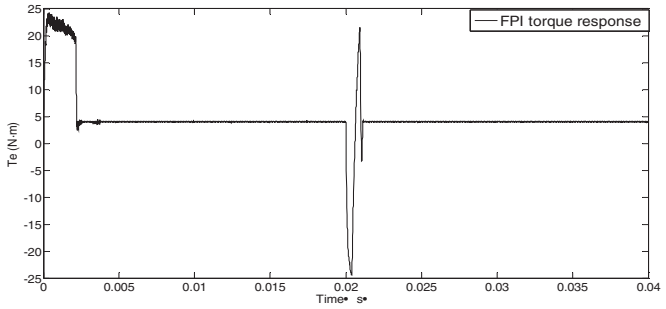

Figure 13. Torque response curve under FPI controller

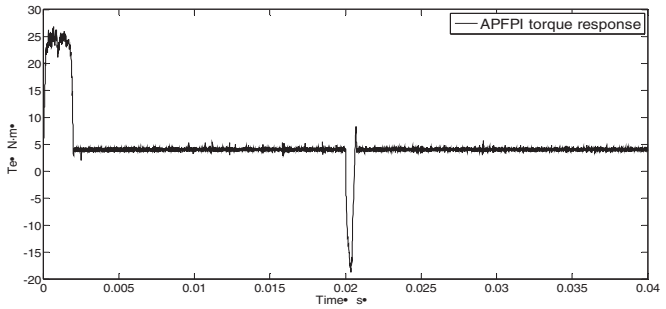

Figure 14. Torque response curve under APFPI controller

Figure 12 to Figure 14 show that the PMSM vector control system with APFPI controller has the best torque control performance. While the command speed changes, the control system with APFPI controller will take shorter time to reach steady-state.

VI. CONCLUSIONS

The PMSM vector control system is a non-linear system. The conventional PI controller which is used in vector control system is not satisfied with the requirements of high precision control. The FPI controller has the prominent advantage in nonlinear system control, and it does not need the precise mathematical model.

A new APFPI controller is proposed in this paper and simulated in the PMSM control system which is built in matlab /simulink. The simulation results suggest that the speed response of PMSM has shorter regulating time and the torque has small ripple. While the command speed changes, the control system with APFPI controller has quick speed tracking performance and small torque ripple. The simulation results show that the new control technique has shown excellent characteristics.

REFERENCES

[1] Risha Na, Xudong Wang, "An improved vector-control system of PMSM based on fuzzy logic controller," 2014 International Symposium on Computer, Consumer and Control, pp. 326-331. June 2014.

[2] M. Azadi, A. Rahideh, A. A. Safavi, and O. Mahdiyar, "Wavenet based vector control of a permanent magnet synchronous motor drive," in Proc. Electric Machines & Drives Conference (IEMDC' 07). IEEE International, vol. 2, pp. 1663–1668, May, 2007.

[3] Garcia, R.C., Suemitsu, W.I., Pinto, J.O.P., "Precise position control of a PMSM based on new adaptive PID controllers," IECON 2011-37th Annual Conference on IEEE Industrial Electronics Society, pp. 1983-1988, Nov. 2011.

[4] M. M. I. Chy and M. N. Uddin, "Development and implementation of a new adaptive intelligent speed controller for IPMSM drive," IEEE Trans. Ind. Appl., vol. 45, no. 3, pp. 1106-1115, May/Jun. 2009.

[5] M. A. S. K.Khan and M. A. Rahman, "A novel neuro-wavelet-based self-tuned wavelet controller for IPM motor drives," in Conf. Rec. IEEE IAS Annu. Meeting, pp. 1-8, Oct, 2008.

[6] D. F. Chen, T. H. Liu, and C. K. Hung, "Nonlinear adaptive backstepping controller design for a matrix-converter based PMSM control system," in Conf. Rec. IEEE-IAS Annu. Meeting, 2003, vol. 1, pp. 673-678.

[7] Jaswant Singh, Bindeshwar Singh, S. P. Singh and Mohd Naim, "Investigation of performance parameters of PMSM drives using DTC-SVPWM technique," 2012 Students Conference on Engineering and Systems, pp. 1-6, March 2012.

[8] C.-M. Lin and C.-F. Hsu, "Supervisory recurrent fuzzy neural network control of wing rock for slender delta wings," IEEE Trans. Fuzzy Systems, vol.12, pp. 733-742, 2004.

[9] Y. Frayman and L.P. Wang, "A dynamically-constructed fuzzy neural controller for direct model reference adaptive control of multi-input-multi-output nonlinear processes," Soft Computing, vol.6, pp.244-253, 2002.

[10] L.P. Wang and Y. Frayman, "A dynamically generated fuzzy neural network and its application to torsional vibration control of tandem cold rolling mill spindles", Engineering Applications of Artificial Intelligence, vol. 15, no. 6, pp. 541-550, December, 2002.

[11] V. Vindhya, V. Reddy, "PID-Fuzzy logic hybrid controller for a digitally controlled DC-DC converter," 2013 International Conference onGreen Computing, Communication and Conservation of Energy, pp. 362-366, Dec 2013.

[12] Limei Wang, Mingxiu Tian, Yanping Gao, "Fuzzy self-adapting PID control of PMSM servo system," IEEE International Electric Machines & Drives Conference, IEMDC '07, pp. 860–863, May 2007.

[13] Yu Cao, Xudong Wang, Risha Na, and Liangliang Mao, "Research on a improved PMSM vector control system," Proceedings of 2011 6th International Forum on Strategic Technology, pp. 678-683, Aug 2011.

[14] Zhou Yilin, Ding Qichen, "Study of PID temperature control for reactor based on RBF network," 2012 IEEE International Conference on Automation and Logistics, pp. 456-460, Aug 2012.

[15] Zeyu Li, Jiangqiang Hu, Xingxing Huo, "PID control based on RBF neural network for ship steering," 2012 World Congress on Information and Communication Technologies, pp. 1076-1080, 2012.